

Study on the Structure and Formation Mechanism of Molybdenum Carbides

Ahmad Hanif, Tiancun Xiao, Andrew P. E. York,[†] Jeremy Sloan, and Malcolm L. H. Green*

Wolfson Catalysis Centre, Inorganic Chemistry Laboratory, University of Oxford, South Parks Road, Oxford OX1 3QR, U.K.

Received April 12, 2001. Revised Manuscript Received November 26, 2001

The synthesis of high-surface-area molybdenum carbides has been studied by the temperature-programmed carburization of molybdenum trioxide MoO₃. The feedstocks used were mixtures of methane and ethane with hydrogen. The solid reaction products were characterized at selected intervals using thermogravimetric analysis differential scanning calorimetry (TGA-DSC), surface area measurement (BET), X-ray diffraction (XRD), and high-resolution transmission electron microscopy (HRTEM). The gaseous products of the carburization process were monitored using a gas chromatograph equipped with a mass spectrometer (GC-MS). The structural properties of the product carbides are shown to depend on the conditions of synthesis. The C₂H₆/H₂ feedstock gave the highest-surface-area material. The presence of H₂ in the feed mixture reduced the amount of amorphous carbon deposited on the molybdenum carbide material. The surface area was found to increase most rapidly during the initial H₂-reduction stage. Initially, the MoO₃ is reduced to form MoO_{3-x}. This material has structural defects, which can account for a decrease in the average particle size and an increased porosity, resulting in an increased surface area. During the carburization process, three phase transitions are observed. At higher temperatures, the rate of deposition of graphitic and amorphous carbons derived from CH₄ or CO is much greater than the rate of hydrogenation of the deposited carbon, resulting in the formation of surface graphitic carbon.

Introduction

The discovery of similarities between the catalytic behavior of group VI transition metal carbides and the noble metals has generated considerable interest.¹ This is due to the possibility for replacing expensive metals, such as Pd, Pt, and Rh, with relatively abundant group VI metals¹⁻⁷ and also to the fact that adsorbed cycloketones on such surfaces are transformed into surface-bound alkylidenes stable to >900 K, which can be used to create a wide range of exceptionally stable organic layers on molybdenum carbide.⁸ Early studies showed that the group VI carbides had good catalytic activities, stabilities, selectivities, and resistances to sulfur poison-

ing. Further, transition metal carbides themselves are not toxic or hazardous materials, because of their high stabilities and insolubility. To optimize the efficiency of these metal carbides, they should have high specific surface areas, S_g . Conventional preparation techniques for metal carbides have been inherited from the metallurgical industry and involve the reaction of metals, metal hydrides, or metal oxides with appropriate amounts of graphitic carbon in a protective or reducing atmosphere. The reaction temperatures are generally high, e.g., >1500 K for Mo₂C. The resulting carbides have a low S_g 's and low purities and are unsuitable for use as catalyst materials.

Several methods have been developed for the preparation of high-surface-area carbides. One of the most widely used methods is the temperature-programmed reduction of the transition metal oxide by gaseous hydrocarbons, as pioneered by Levy and Boudart.¹ It has been shown that use of higher flow rates of the gas mixture give carbide materials with a higher S_g values.^{9,10} Also, the structure of the carbide can be controlled through preactivation in hydrogen or the use of hydrogen/hydrocarbon mixtures. The presence of added H₂ in the feed mixture reduces the amount of carbon deposited and increases the S_g of the resulting carbides. The presence of hydrogen gives rise to the formation of

* Author to whom correspondence should be addressed: Prof. M. L. H. Green, Inorganic Chemistry Laboratory, University of Oxford, South Parks Road, Oxford, OX1 3QR, U.K. Tel.: +44-1865-272649. Fax: +44-1865-272690. E-mail: malcolm.green@chem.ox.ac.uk.

[†] Current address: Johnson Matthey Technology Centre, Blount's Court, Sonning Common, Reading RG4 9NH, U.K.

- (1) Levy, R. B.; Boudart, M. *Science* **1973**, *181*, 547.
- (2) Ribeiro, F. H.; Boudart, M.; Dalla Betta, R. A.; Iglesia, E. *J. Catal.* **1991**, *130*, 498.
- (3) Sinfelt, J. H.; Yates, D. C. *J. Nat. Phys. Sci.* **1971**, *27*, 229.
- (4) Chen, J. G. *Chem. Rev.* **1996**, *96*, 1477.
- (5) Ledoux, M. J.; Pham-Huu, C.; Guille, J.; Dunlop, H.; Hantzer, S.; Marin, S.; Weibel, W. *Catal. Today* **1992**, *15*, 263.
- (6) Bécue, T.; Manoli, J.-M.; Potvin, C.; Davis, R. J.; Djéga-Mariadassou, G. *J. Catal.* **1999**, *186*, 110.
- (7) Bouchy, C.; Schmidt, I.; Anderson, J. R.; Jacobsen, C. J. H.; Derouane, E. G.; Derouane-Abd Hamid, S. B. *J. Mol. Catal. A: Chem.* **2000**, *163*, 283.
- (8) El Zahhidli, M.; Oudghiri-Hassani, H.; McBreen, P. H. *Nature* **2001**, *409*, 1023.

(9) Brungs, A. J. D. Philos. Thesis, Inorganic Chemistry Laboratory, University of Oxford, Oxford, U.K., 1998.

(10) Choi, J. G. *Appl. Catal. A* **1999**, *184*, 189.

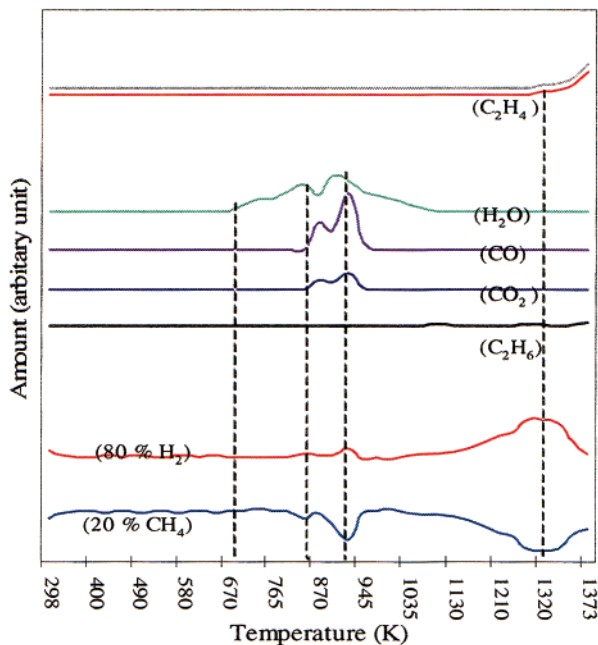


Figure 1. TPR-GC-MS profiles of carburization of MoO_3 by 20% CH_4/H_2 .

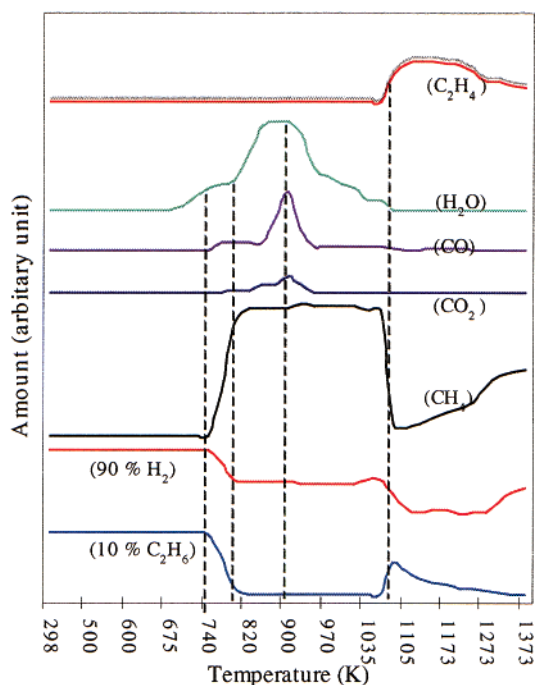


Figure 2. TPR-GC-MS profiles of carburization of MoO_3 by 10% $\text{C}_2\text{H}_6/\text{H}_2$.

the oxycarbide ($\text{MoO}_{2.4}\text{C}_{0.2}\text{H}_{0.8}$) from MoO_3 and leads to topotactic formation of new materials. In the absence of H_2 , only nontopotactic formation of MoO_2 is observed.¹¹

It has been shown that the choice of the hydrocarbon reactant can influence both the structure and the resulting catalytic performance of the product carbides.^{12–18} Ranhotra et al.¹² found that ethane hydro-

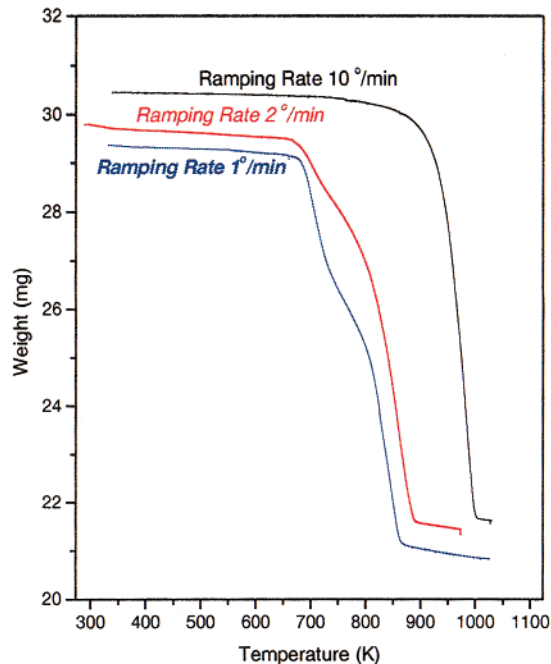


Figure 3. TGA profiles of carburization of MoO_3 using 10% $\text{C}_2\text{H}_6/\text{H}_2$ at different heating rates.

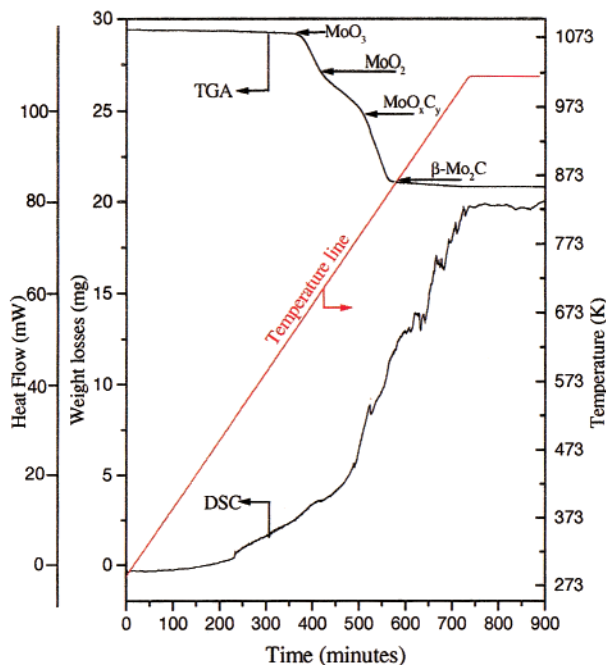


Figure 4. TGA-DSC curves during the carburization process at 1 K/min.

genolysis over MoO_3 at 573 K was more effective than pretreatment with a CH_4/H_2 mixture at 623 K in

(11) Bouchy, C.; Pham-huu, C.; Ledoux, M. J. *J. Mol. Catal. A: Chem.* **2000**, *162*, 317.

(12) Ranhotra, G. S.; Haddix, G. W.; Bell, A. T.; Reimer, J. A. *J. Catal.* **1987**, *108*, 24.

(13) Bouchy, C.; Hamid, B. D.-A.; Derouane, E. G. *Chem. Commun.* **2000**, 125.

(14) Claridge, J. B.; York, A. P. E.; Brungs, A. J.; Green, M. L. H. *Chem. Mater.* **2000**, *12*, 132.

(15) Xiao, T.-C.; York, A. P. E.; Williams, V. C.; Al-Megren, H.; Hanif, A.; Zhou, X.-Y.; Green, M. L. H. *Chem. Mater.* **2000**, *12*, 3896.

(16) Oyama, S. T.; Delporte, P.; Pham-Huu, C.; Ledoux, M. *J. Chem. Lett.* **1997**, 949.

(17) Löfberg, A.; Frennet, A.; Leclercq, G.; Leclercq, L.; Giraudon, J. M. *J. Catal.* **2000**, *189*, 170.

(18) York, A. P. E.; Claridge, J. B.; Williams, V. C.; Brungs, A. J.; Sloan, J.; Hanif, A.; Al-Megren, H.; Green, M. L. H. *Stud. Surf. Sci. Catal.* **2000**, *130B*, 989.

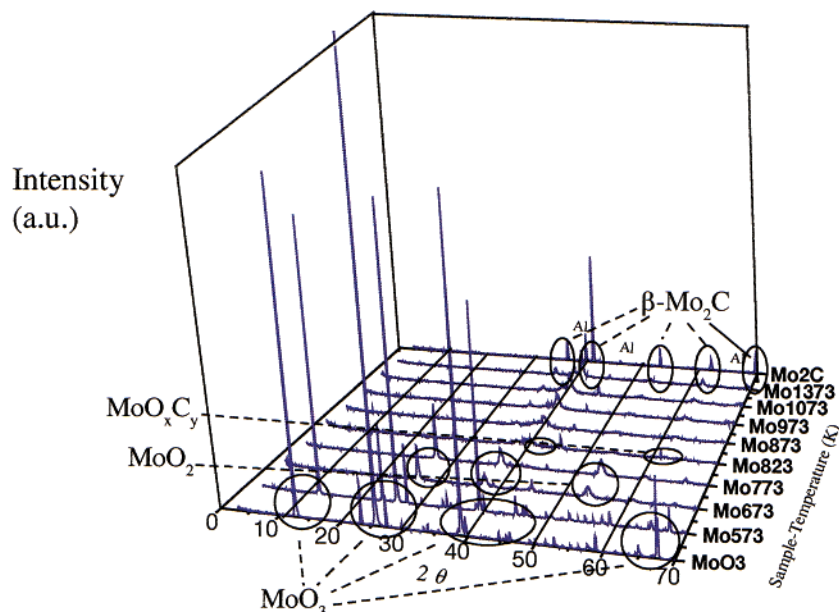


Figure 5. XRD patterns at different temperatures after MoO_3 carburization with 20% CH_4/H_2 .

removing oxygen from the bulk of MoO_3 . Bouchy et al.¹³ showed that the prerduction of MoO_3 with pure hydrogen followed by carburization with a mixture of CH_4/H_2 leads to a metastable fcc molybdenum carbide. Claridge et al.¹⁴ reported that replacement of methane by ethane for carburization leads to carbides with higher surface areas because they are formed at lower temperatures. Few studies have been reported on the phase transitions occurring during the carburization and on the mechanism of formation of the molybdenum carbide. In this paper, molybdenum carbides were prepared using several different hydrocarbons and characterized using the TPR techniques. The purpose was to gain insight into the mechanism of carbide formation and to achieve carbide materials with higher surface areas and also improved pore size distributions.

Experimental Section

Sample Preparation. The oxide MoO_3 (200 mg) (Alfa, 99.999% purity) was placed in a 9-mm (o.d.) silica tube plugged with silica wool at both ends. Carburizing reagents were either 20% CH_4/H_2 or 10% $\text{C}_2\text{H}_6/\text{H}_2$ and were passed over the molybdenum oxide at flow rates varying between 100 and 120 mL min^{-1} and at ramping rates of 1 K min^{-1} . The exit gas products were analyzed using an on-line GC-MS (HP 5890) equipped with TCD and FID detectors. In serial experiments, the carburization temperatures were increased in 50–100 K steps from 523 to 1373 K and held at each temperature for 2 h. After carburization, the samples were cooled to room temperature under an argon flow. Before being exposed to air, the carbide product was passivated by treatment with a flow of 1 vol % O_2/N_2 at room temperature for 2 h.

The resulting carbides were studied immediately to limit further oxidation of the catalyst. The surface area measurements of the samples were performed in a glass BET apparatus. The crystalline components of the materials were examined by X-ray diffraction (XRD) using a Philips PW1710 diffractometer equipped with $\text{Cu K}\alpha$ radiation. A JEOL-4000EX high-resolution electron microscope with an accelerating voltage of 400 kV was used to observe the morphology and microstructure of the product materials.

Crystallite sizes of the product carbides were established from the XRD data using the Scherrer equation, $D_c = 0.9\lambda/$

$(\beta \cos \theta)$, where λ is the wavelength of the X-ray radiation (0.154 nm), β is the width of the peak at half-maximum corresponding to the $\{200\}$ plane and corrected for instrumental broadening (0.1°), and θ is the Bragg angle. Corresponding particle sizes were calculated from the equation $D_p = 6/(\rho S_g)$, where ρ is the density of the solid and S_g is the specific surface area of the sample, which was measured by BET.

The changes in the MoO_3 sample during carburization were monitored by thermogravimetric analysis (TG, Rheometric Scientific STA 1500). A sample of 30 mg of MoO_3 was loaded into a small platinum crucible, and the heating rate was 2 K/min under an atmosphere of 20% CH_4/H_2 or 10% $\text{C}_2\text{H}_6/\text{H}_2$. The upper limit of temperature used for the measurements was 1023 K, and this was maintained for 2 h.

Results and Discussion

Carburization of Molybdenum Trioxide with 20% CH_4/H_2 and 10% $\text{C}_2\text{H}_6/\text{H}_2$. Figure 1 shows the changes in the product gases during temperature-programmed reduction of MoO_3 using 20% CH_4/H_2 . It can be seen that water starts to form between 670 and 700 K and that it is produced while methane is not yet involved in the reaction. Below 750 K, therefore, only hydrogen is involved in the early stages of the reduction of the oxide. At about 870 K, the methane concentration starts to decrease, and corresponding peaks for CO_2 , CO, and water are observed. This indicates that methane is acting both as the carbon source and also as a reductant. Similar results were reported for the TPR of molybdenum oxides using 20% CH_4/H_2 above 950 K.^{14,19} There are two peaks for CO and CO_2 production (870 and 920 K), and at the same time, two peaks for hydrogen, suggesting that carburization has occurred. Methane is involved in the reduction and carburization of MoO_3 to produce more hydrogen during the carburization. After the two peaks for CO and CO_2 appeared, an increasing amount of hydrogen was observed, along with a correspondingly increased consumption of CH_4 . In addition, the peaks for CO_x and water diminished, indicating that

(19) Lee, J. S.; Yeom, M. H.; Park, K. Y.; Nam, I.-S.; Chung, J. S.; Kim, Y. G.; Moon, S. H. *J. Catal.* **1991**, *128*, 126.

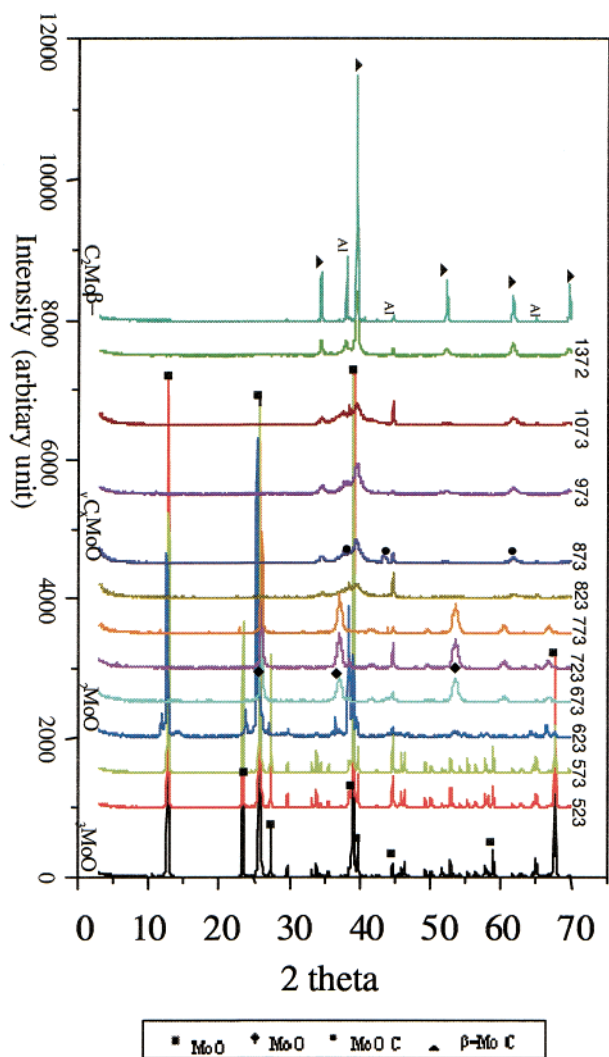


Figure 6. XRD patterns of MoO_3 carburized with 10% $\text{C}_2\text{H}_6/\text{H}_2$ at different temperatures.

carbon was being deposited on the catalyst surface. Above 1320 K, the production of hydrogen decreased, and some CH_4 was converted into C_2H_4 and a small amount of C_2H_6 .

When ethane was used as the carbon source (Figure 2), the first water product peak appeared at almost the same temperature as for CH_4 , indicating that the behavior of hydrogen in the two systems is similar, as would be expected. This first stage of hydrogen reduction was followed at 740 K by C_2H_6 hydrogenolysis to produce CH_4 . At 800 and 900 K, both reduction and carburization occurred, as indicated by GC-MS peaks for CO_2 , CO , and water, formed by the reaction of molybdenum oxides with ethane or possibly methane. Compared to methane, ethane was found to be more active in the reduction process. The hydrogenolysis of ethane was complete at 1070 K, while further reduction of the molybdenum oxide by ethane also occurs. Finally, some of the ethane is dehydrogenated to give ethylene and hydrogen; some is also hydrogenolysed to give methane.

Changes in the Molybdenum Oxide during Carburization. The carburization process of MoO_3 using methane was studied by TGA-DSC as reported elsewhere.¹⁸ Here, we present TGA-DSC studies during the

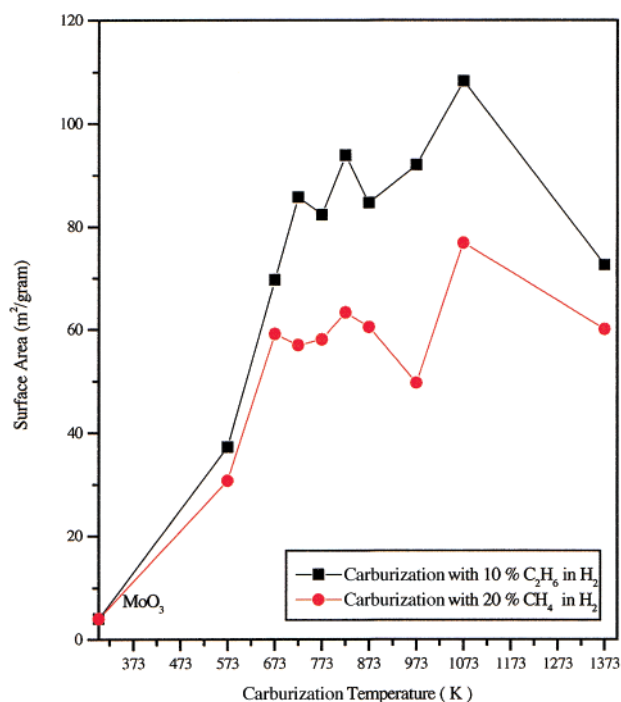


Figure 7. Surface areas of molybdenum carbide prepared using 20% CH_4/H_2 and 10% $\text{C}_2\text{H}_6/\text{H}_2$ carburization at different temperatures.

course of the carburization of MoO_3 to Mo_2C using 10% ethane in hydrogen as a feedstock at atmospheric pressure with different ramping rates. The data from these experiments are shown in Figure 3.

At the ramping rate of 10 K min^{-1} , the initial MoO_3 material was transformed to Mo_2C in one step in the temperature range 870–1000 K. However, when the ramping rate was decreased to 2 K min^{-1} , the carburization commenced at a much lower temperature (650 K), and a transition point at 770 K was clearly observed. With a ramping rate of 1 K min^{-1} , three weight-loss stages occurred during the carburization reaction at 670, 800, and 920 K. These are shown in more detail in Figure 4. At 670 K, the heat flow changed, and the MoO_3 weight loss was 11%, indicating the formation of MoO_2 . At 800 K, a weight loss of 17.7% was found, suggesting that a molybdenum oxycarbide [MoO_xC_y , $(x + y) < 1$] was formed. Finally, above 920 K, a total weight loss of 29.5% indicated that the molybdenum oxycarbide was converted to the molybdenum carbide Mo_2C . The DSC curves show that the carburization steps are endothermic; a small exothermic reaction occurs over the range of 920 and 970 K, probably due to the effect of reduction and formation of Mo–C bonds.

XRD Study of Structure Transformations during Carburization. The bulk structures of the molybdenum material during carburization with 20% CH_4/H_2 and 10% $\text{C}_2\text{H}_6/\text{H}_2$ were determined at temperature steps of between 50 and 100 K by XRD. Figure 5 shows the diffraction patterns of the molybdenum carbides obtained using 20% CH_4/H_2 ; the diffraction peaks of the most prominent phases have been assigned. A comparison between the experimental and literature data is provided in Table 1.

At 673 K, after the first reduction of MoO_3 , a typical XRD pattern for monoclinic MoO_2 was observed. This result is in agreement with literature results for the

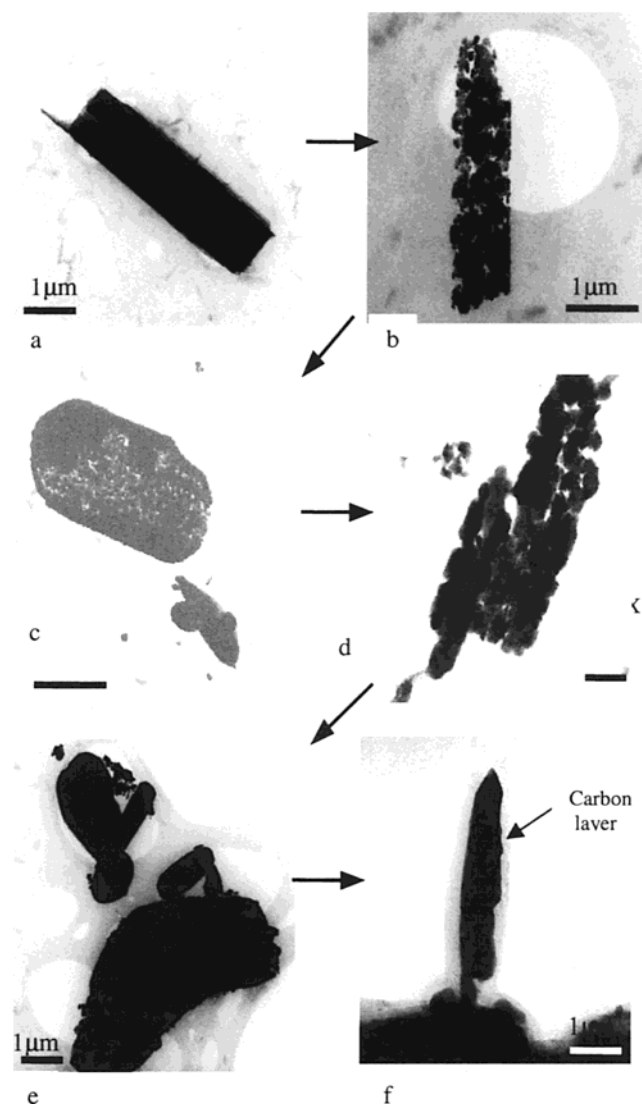


Figure 8. (a–f) Sequence of TEM images of molybdenum carbide prepared using 10% C_2H_6/H_2 carburization at different temperatures

reduction of MoO_3 to Mo metal using hydrogen or 20% CH_4/H_2 .^{20,21}

The first carburization of MoO_2 occurred at 823 K, leading to a transition species that is probably a molybdenum oxycarbide, MoO_xC_y , which has a face-centered-cubic (fcc) structure, as observed by Ledoux who used a TPR method with a feedstock of 0.7% hexane in hydrogen at high pressure and a temperature of 623 K.¹⁶ The second carburization step started at 873 K and ended at 973 K; it gave some β - Mo_2C , and MoO_xC_y was still apparent. Above 973 K, all traces of oxides disappeared, and pure hexagonal-close-packed (hcp) or β - Mo_2C was formed.^{14–16,18,21–23} The diffraction peaks for β - Mo_2C were much sharper at higher carburization temperatures, suggesting that the particle size within these samples was significantly larger. (See Table 2.)

(20) Arnoldy, P.; de Jonge, J. C. M.; Moulijn, J. A. *J. Phys. Chem.* **1985**, *89*, 4517.

(21) Tutiya, H. *Bull. Inst. Chem. Res., Kyoto Univ.* **1932**, *11*, 1150.

(22) Lee, J. S.; Volpe, L.; Ribeiro, F. H.; Boudart, M. *J. Catal.* **1988**, *112*, 44.

(23) Lee, J. S.; Locatelli, S.; Oyama, S. T.; Boudart, M. *J. Catal.* **1990**, *125*, 157.

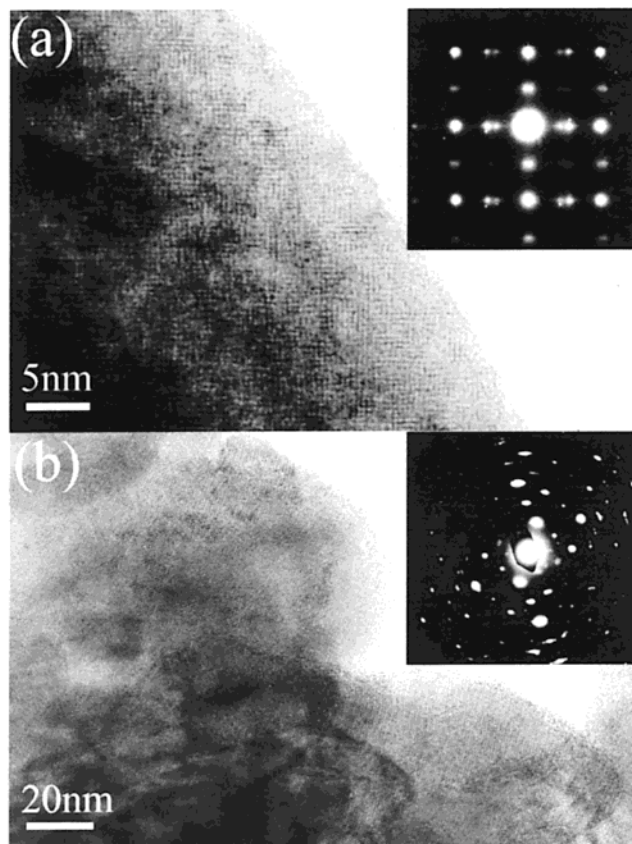


Figure 9. Micrographs showing the product of ethane TPR of (a) single-crystalline MoO_3 at 623 K and (b) polycrystalline MoO_3 at 673 K.

Table 1. Comparison between XRD Data for Molybdenum Oxide and Carbides Found during Carburization Using 20% CH_4/H_2 and Standard Data

compound	measurement	literature data
	2θ ($^\circ$) (intensity/%)	2θ ($^\circ$) {plane}
MoO_3 (precursor)	25.71 (100), 12.76 (66),	25.7 {040}, 12.8 {020},
	39.00 (47), 67.5 (8),	39.0 {131}, 67.5 {0100},
	23.3 (7), 27.3 (5)	23.3 {110}, 27.3 {021}
MoO_2 (673 K)	26.0 (100), 37.0 (30),	26.0 {−111}, 37.0 {−211},
	53.54 (26)	53.5 {−312}
MoO_xC_y (823 K)	44.1 (100), 62.9 (71),	43.6 {200}, 37.5 {111},
	37.1 (55)	63.5 {220}
β - Mo_2C (973 K)	39.46 (100), 38.00 (25),	39.5 {101}, 37.9 {002},
	34.4 (20) 52.24 (18),	34.5 {100} 52.2 {102},
	69.6 (15), 61.5 (10)	69.6 {103}, 61.6 {110}

Figure 6 shows XRD patterns of molybdenum oxide carburized with 10% C_2H_6/H_2 at different temperatures. The XRD patterns appear to be similar to those for carburization using methane; however, the temperatures at which the reactions occurred were lower, indicating that ethane was more active for reducing the molybdenum trioxide. The new observed peaks were broad and weak. This suggests that the molybdenum intermediates and the molybdenum carbide particles from the ethane system were smaller than those from methane.

Surface Area Changes of Molybdenum Oxide and Carbide during Carburization. The changes in the surface area of MoO_3 with carburization temperature are shown in Figure 7. The molybdenum trioxide initially had a low surface area of below $5 \text{ m}^2 \text{ g}^{-1}$. However, after treatment with a mixture of methane/

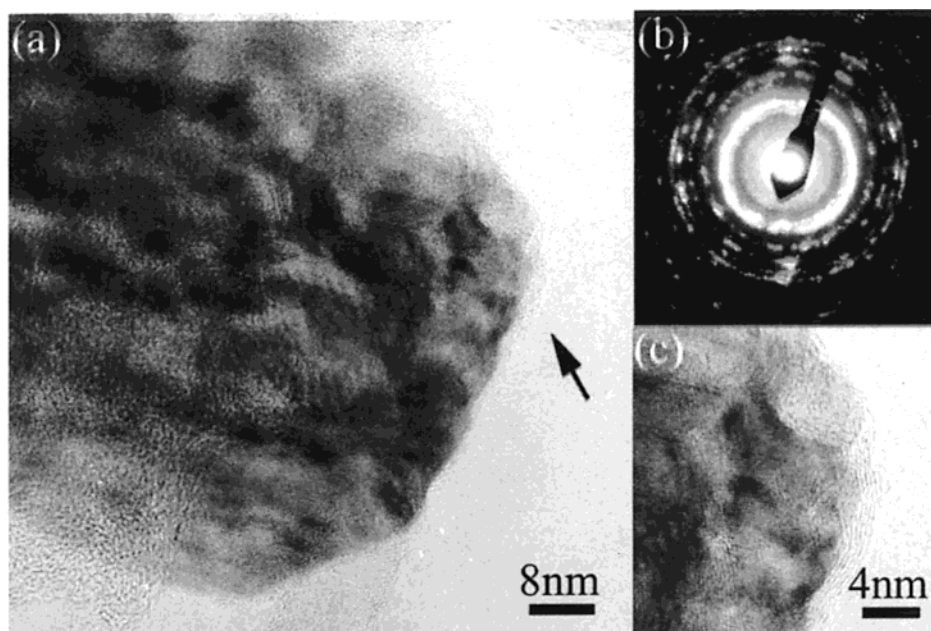


Figure 10. (a) Low-magnification TEM of Mo₂C following complete carburization, (b) ED ring pattern corresponded to Mo₂C, (c) detail from a following carbon layer formation on carbide surface.

Table 2. Comparison of the Particle Sizes of the Molybdenum Oxide and Carbides Derived from XRD and BET Isotherms for a Temperature-Programmed Reaction

compound	TPR temp (K)	r_{200}^a (nm)	S_g (m ² g ⁻¹)	r_{BET}^b (nm)
TPR with CH ₄ /H ₂				
precursor MoO ₃ (Alfa JM)		100.280	<5	150.914
MoO ₂	673	11.010	59	7.859
MoO ₂	723	8.887	57	8.135
MoO ₂ (+ MoO _x C _y)	773	9.773	58	7.389
MoO _x C _y (+ β-Mo ₂ C)	823	6.543	63	5.952
β-Mo ₂ C (+ MoO _x C _y)	873	5.364	60	5.618
β-Mo ₂ C	973	7.556	49	6.879
β-Mo ₂ C	1073	10.230	76	4.435
β-Mo ₂ C	1373	36.270	60	11.236
TPR with C ₂ H ₆ /H ₂				
precursor MoO ₃ (Alfa JM)		100.280	<5	150.914
MoO ₃ (+ MoO ₂)	623	12.136	50	10.000
MoO ₂	673	6.065	70	6.624
MoO ₂	723	5.735	86	5.392
MoO ₂	773	6.111	82	5.226
MoO _x C _y (+ β-Mo ₂ C)	823	3.270	94	3.990
β-Mo ₂ C (+ MoO _x C _y)	873	4.681	95	3.547
β-Mo ₂ C	973	6.885	92	3.664
β-Mo ₂ C	1073	9.705	108	6.242
β-Mo ₂ C	1373	18.254	73	9.235

^a $r_{200} = D_c/2 = [0.9\lambda/(\beta \cos \theta)]/2$ from XRD. ^b $r_{BET} = D_p/2 = [6/(\rho S_g)]/2$ from BET.

H₂ or ethane/H₂, even at 573 K (according to the TPR-MS results, the carbon source is not yet involved in the reduction), the surface area increased to 30 and 37 m² g⁻¹ for methane and ethane, respectively. This implies that the particles of MoO₃ were being reduced, leaving more oxide surface exposed. This finding is in agreement with the results of Ledoux et al.,¹⁶ who reported the formation of a high- S_g oxycarbide of molybdenum at temperatures as low as 623 K after TPR of MoO₃ using 0.7% *n*-hexane in hydrogen. We conclude that the early reduction stage of MoO₃ occurs with hydrogen alone and causes a rapid increase in the surface area. As we have reported,¹⁵ this increase in surface area might be due

to cracking and degradation of the initially smooth MoO₃ crystal surface.

After hydrogen reduction at 673 K, the surface area increased rapidly to 59 and 70 m² g⁻¹ for methane and ethane, respectively. During this stage, the TPR-MS data (Figure 3) showed that hydrogen had reduced MoO₃ to form MoO₂ and water. With further reduction, the surface area was relatively constant at first and then rose again at 823 K as carburization took place. The surface area increased very quickly at 1073 K to 110 m² g⁻¹, in the case of ethane, and the β-Mo₂C (hcp) had formed. The surface area of the molybdenum carbide decreased at higher temperatures (> 1123 K) as a result of sintering and, to a greater extent, the deposition of carbon on the surface of the catalyst.

Figure 7 also shows that the surface area of the molybdenum carbide prepared using the mixture of ethane and hydrogen is higher than that obtained when methane/H₂ is used. Previous studies^{24,25} have shown that the Mo₂C prepared using ethane/H₂ has smaller particles and a rougher surface.

High-resolution transmission electron microscopy (HRTEM) morphologies for molybdenum carbides formed during the TPR studies using 10% ethane/H₂ at different temperatures are shown in Figure 8a–f.

The initial MoO₃ crystals had a needlelike structure, with each needle being 2–7 μm long. After reduction in ethane/hydrogen at 673 K, the resulting MoO₂ crystals were converted to smaller crystal clusters of about 0.1–0.3 μm in diameter. This helps to explain the rapid increase in the surface area. After reductions at 623 and 673 K, the product was studied by electron diffraction (Figure 9), and two different structures can be seen: (a) single crystals of rhombic MoO₃ and (b) ring patterns due to polycrystalline MoO₂.

(24) Xiao, T.; York, A. P. E.; Coleman, K. S.; Claridge, J. B.; Sloan, J.; Charnock, J.; Green, M. L. H. Effect of carburising agent on the structure of molybdenum carbides. *J. Mater. Chem.* **2001**, *11*, 3094.

(25) Choi, J. S.; Bugli, G.; Djega-Mariadassou, G. *J. Catal.* **2000**, *193*, 238.

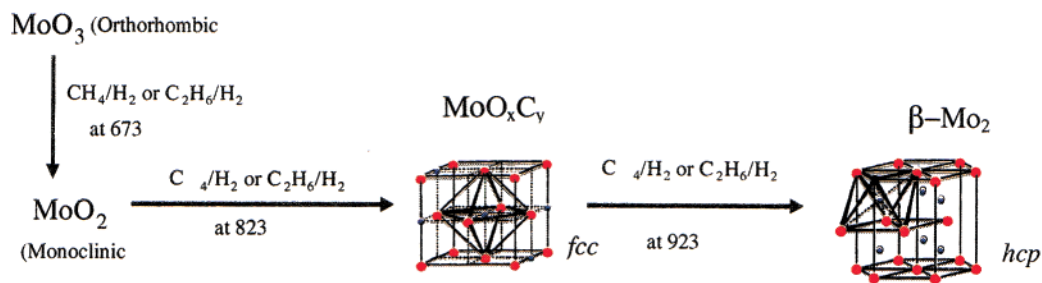


Figure 11. Routes to the various molybdenum carbide phases via TPR.

After carburization at 823 K, the surface of the particles became further rougher, and XRD and electron diffraction results show that the crystalline phase was cubic MoO_xC_y . Figure 8d shows that the particles were further degraded to become looser and rougher when carburized to 973 K, and the electron diffraction pattern of the product indicates that the hexagonal $\beta\text{-Mo}_2\text{C}$ had been formed. Also, small pores or channels were present in the $\beta\text{-Mo}_2\text{C}$, and the surface of the molybdenum carbide became rougher, which might be the reason for the rapid increase in measured surface area. When the carburization temperature was raised to 1073 K, the surface morphology of the resulting molybdenum carbide materials changed as shown in Figure 8e. In Figure 10a–c, one can see that the particle surface became condensed, suggesting that the crystal particles aggregated, and that the surface area was further decreased (as shown in Figure 7), as the carbon layers on the surface of carbide had become thicker. The HRTEM images (Figures 8f and 10c) of the TPR material at 1373 K show that the deposited carbon formed a multilayered material on the surface of the carbide that completely covered all of the Mo_2C catalysts.

Figure 11 shows that three phases are involved during the carburization of molybdenum trioxide. MoO_2 and MoO_xC_y are shown as intermediates in the transformation of MoO_3 to Mo_2C .

Conclusions

TPR studies coupled with HRTEM, XRD, and BET measurements have provided more evidence to explain the observation that the reduction of MoO_3 by $\text{C}_2\text{H}_6/\text{H}_2$ gives the $\beta\text{-Mo}_2\text{C}$ with the highest obtained surface area. Intermediate MoO_2 and MoO_xC_y phases were clearly observed during the carburization of MoO_3 using both CH_4/H_2 and $\text{C}_2\text{H}_6/\text{H}_2$. Carburization of MoO_3 above 1073 K caused reduction of the surface area by sintering and condensed carbon deposition on the carbide surface.

Acknowledgment. T.X. is a Royal Society BP-Amoco fellow from Shandong University, China. We thank Pertamina for financial support for A.H. and CANMET for financial support for A.P.E.Y., as well as the Royal Society for RSURF (to J.S.).

CM011096E